RSC Advances

PAPER

View Article Online
View Journal | View Issue

Cite this: *RSC Adv.*, 2024, **14**, 32818

Biomimetic nanoparticles with red blood cell membranes for enhanced photothermal and immunotherapy for tumors†

Liquan Hong,[a] Jingtao Ye,[b] Yang Li[b] and Shouchun Yin *[ab]

The alarming escalation in cancer incidence and mortality has thrust into spotlight the quest for groundbreaking therapeutic strategies. Our research delves into the potential of RDIR780, a novel class of biomimetic nanoparticles cloaked in red blood cell membranes, to significantly enhance their *in vivo* persistence and therapeutic potency. Through an exhaustive suite of experiments, we have charted the therapeutic horizons of RDIR780 in the realms of tumor photothermal synergistic immunotherapy and targeted drug delivery. Preliminary *in vitro* cellular assays have revealed that RDIR780 not only achieves remarkable uptake by tumor cells but also triggers swift tumor cell death under the influence of laser irradiation. Subsequent *in vivo* fluorescence imaging studies have corroborated the nanoparticles' propensity for tumor-specific accumulation, thereby bolstering the case for precision medicine. The results of the precise imaging techniques of therapeutic trials conducted on mice with implanted tumors have underscored the profound impact of RDIR780 when synergized with an anti-PD-L1 antibody. This synergistic approach has shown to fairly eradicate tumor growth, marking a significant stride in the battle against cancer. This pioneering endeavor not only lays down a formidable groundwork for the evolution of long-circulating photothermal therapeutic nanoparticles but also heralds a new era of transformative clinical interventions.

Received 27th September 2024
Accepted 30th September 2024

DOI: 10.1039/d4ra06965j

rsc.li/rsc-advances

1. Introduction

In the forefront of oncology, groundbreaking treatment modalities like photothermal therapy (PTT),[1] photodynamic therapy (PDT),[2–4] chemodynamic therapy (CDT),[5,6] and immunotherapy have garnered considerable acclaim for their innovativeness and therapeutic prowess.[7] PTT, with its non-invasive and highly specific approach,[8] has risen to prominence for its ability to convert light energy into heat, thereby selectively destroying cancer cells with minimal side effects. The strategic use of near-infrared light in PTT, renowned for its low absorption and scattering in biological tissues, has become a cornerstone of this therapeutic approach.[9,10] Evidences suggest that PTT incites the intrinsic apoptotic pathway, leading to cell death.[11] Yet, the effectiveness of PTT in combating metastatic and recurrent tumors is constrained, underscoring the imperative for multimodal therapeutic integration.[12]

Immunotherapy, which harnesses the body's innate immune defenses to eradicate malignant cells, confronts challenges such as immune evasion and the subversion of T-cell signaling by cancer.[13–18] The 2018 Nobel Prize in Medicine, awarded for breakthroughs in immunotherapy, catalyzed a surge in research and clinical applications. Cytokine therapies like interleukin-2 (IL-2) and interferon-α (IFN-α), cell-based therapies, and immune checkpoint blockade targeting cytotoxic T-lymphocyte associated protein 4 (CTLA-4), programmed cell death protein 1 (PD-1), and programmed cell death ligand 1 (PD-L1) strategies have significantly bolstered the anti-tumor response and fostered enduring memory effects that are crucial for preventing tumor metastasis and recurrence.[19–23] Despite these strides, the quest for therapeutic consistency and cancer specificity in immunotherapy continues, with the potential for immune-related adverse effects.[24,25] To surmount these hurdles, the amalgamation of immunotherapy with targeted treatments like PTT is being explored to refine therapeutic efficacy and curtail side effects.

The quest to overcome the limitations of photothermal agents, such as solubility, stability, and tumor site accumulation, has spurred the innovation of nano-carriers, including liposomes, polymer micelles, and mesoporous silica nanoparticles.[26,27] The strategic modification of surface ligands on these nanoparticles enables specific binding to tumor cell receptors, while the use of cell membrane-coated nanoparticles facilitates active targeting.[28,29] This targeted delivery paradigm elevates the concentration of photothermal agents at the tumor site. Our preliminary research encapsulated the photothermal agent IR-780 within the amphiphilic polymer 1,2-dioleoyl-*sn*-glycero-3-phosphoethanolamine-poly(ethylene glycol) (DSPE-

[a]*Deqing Hospital of Hangzhou Normal University, The Third People's Hospital of Deqing, Deqing, 313200, China. E-mail: yinsc@hznu.edu.cn*

[b]*Key Laboratory of Organosilicon Chemistry and Materials Technology of Ministry of Education, College of Materials, Chemistry and Chemical Engineering, Hangzhou Normal University, Hangzhou 311121, China*

† Electronic supplementary information (ESI) available. See DOI: https://doi.org/10.1039/d4ra06965j

PEG-OH), yielding DSPE-PEG-OH@IR-780 (DIR780) nanoparticles.[30] These were further enveloped with red blood cell membranes (RBCM) derived from murine blood, culminating in the creation of biomimetic RBCM@DSPE-PEG-OH@IR-780 (RDIR780) nanoparticles endowed with immune-evasive capabilities. RDIR780 exhibits a remarkable photothermal conversion efficiency of up to 27.8%, coupled with exceptional stability and prolonged blood circulation. Capitalizing on the immune-evasive cluster of differentiation 47 (CD47 protein) present on the red blood cell membrane, we anticipate an enhancement in drug circulation and an increase in drug accumulation at the tumor site. Utilizing fluorescence imaging technology, we meticulously monitored the biodistribution of these biomimetic nanoparticles in mice, identifying the optimal laser irradiation duration to maximize therapeutic efficacy (Scheme 1). Moreover, we synergized RDIR780 with PD-L1 antibodies to assess the combined antitumor potency of this photothermal-immunotherapy alliance in *in vitro* and *in vivo* tumor models. This research pioneers a novel paradigm for the design of tumor-targeted synergistic cancer therapies and introduces a promising strategy for the development of nano-drug carriers that are both immune-evasive and exhibit enhanced retention at the tumor site.

2. Experimental section

Materials, cellular uptake, *in vitro* cell viability, detection of immunogenic cell death (ICD) biomarkers, *in vivo* fluorescence imaging, *in vivo* anti-tumor, and immunohistochemical analyses are detailed in the ESI.†

3. Results and discussion

3.1 Cellular uptake and cytotoxicity

The crux of the therapeutic efficacy of DIR780 and RDIR780 in subsequent experimental endeavors is predicated upon their efficacious cellular internalization. To validate this, we embarked on an initial assessment of the cellular uptake of these agents. 4T1 cells were cultured in DMEM enriched with DIR780 or RDIR780, with subsequent nuclear delineation achieved through DAPI staining to pinpoint cellular location. Under the scrutiny of confocal laser scanning microscopy (CLSM), the red fluorescence of IR780 was observed to encircle the nuclei demarcated by blue DAPI fluorescence (Fig. 1a), an unequivocal testament to the successful internalization of DIR780 and RDIR780 by 4T1 cells. In a parallel series of experiments, 4T1 cells were exposed to the DIR780 or RDIR780-laden medium for varying durations, culminating in flow cytometry analysis. As illustrated in Fig. 1b and c, the uptake of DIR780 or RDIR780 by 4T1 cells escalated with time, with RDIR780 manifesting a more pronounced uptake than DIR780. These observations suggest that the meticulously crafted RDIR780 possesses considerable potential for biological applications.

Delving deeper into the *in vitro* therapeutic effects of RDIR780, our findings, as delineated in Fig. 1d, reveal that at concentrations below 0.8 μg mL^{-1}, RDIR780 exerts negligible cytotoxicity. We

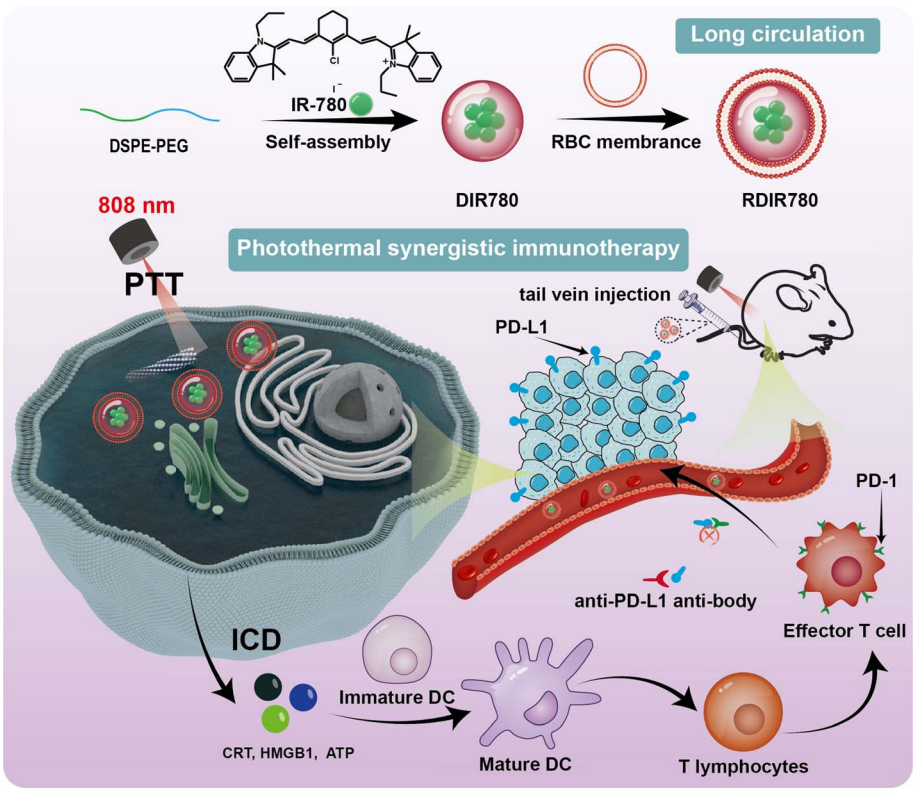

Scheme 1 Schematic of the preparation of RDIR780 and its synergistic photothermal and immunotherapeutic effects.

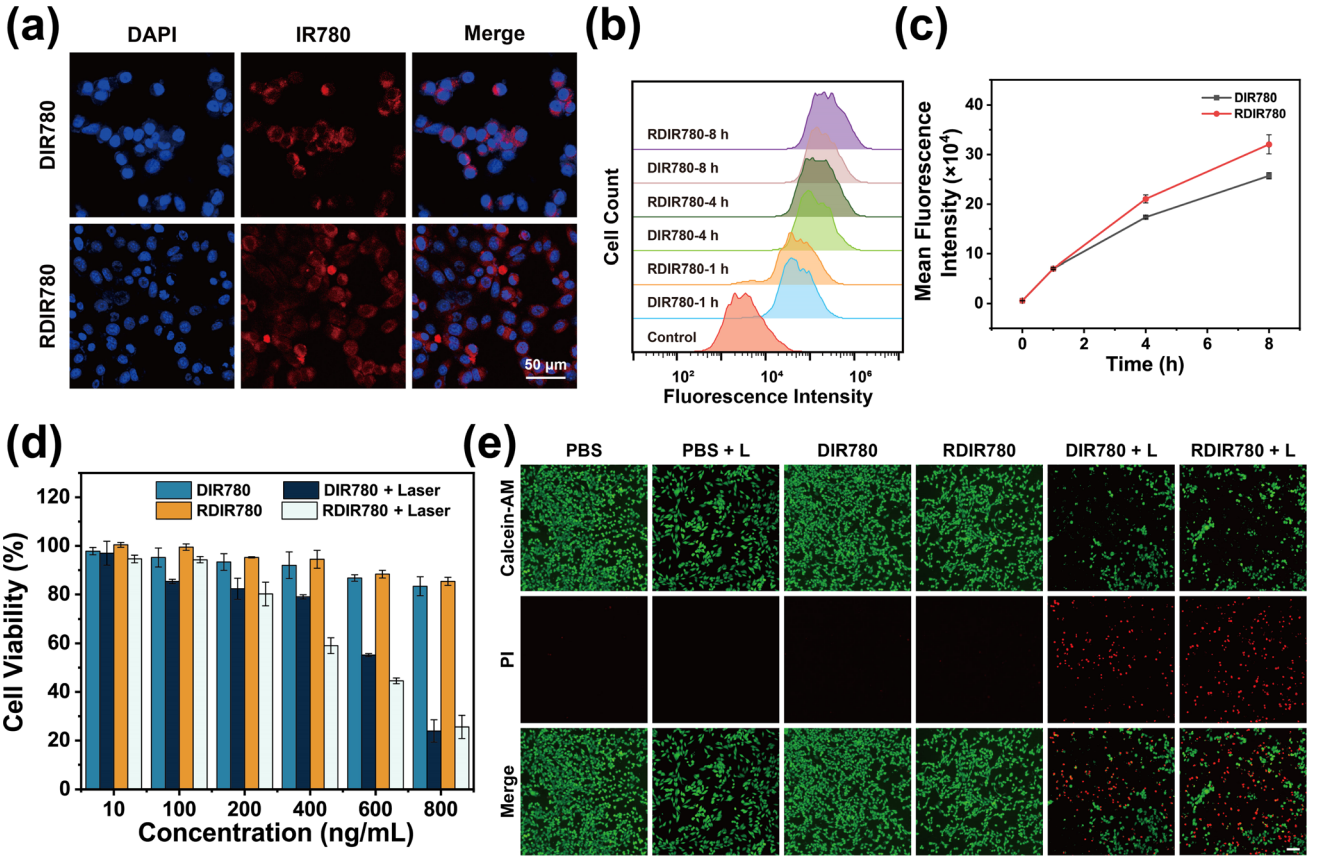

Fig. 1 (a) Confocal images of cell uptake of DIR780 and RDIR780. The 4T1 cell nucleus was stained with DAPI (scale bars: 50 μm). (b) Histogram of flow cytometry after co incubation of DIR780 and RDIR780 with 4T1 cells for different time periods. (c) Signal changes of DIR780 and RDIR780 in 4T1 cells over time. (d) Cell survival rates at different concentrations of DIR780 and RDIR780 with 4T1 cells under dark conditions and after 808 nm laser irradiation (1.0 W cm^{-2}). (e) Staining images of living/dead cells of DIR780 and RDIR780 and 4T1 cells under dark conditions or after 808 nm laser irradiation (1.0 W cm^{-2}) (scale: 50 μm).

meticulously calibrated the laser irradiation duration to ensure that it was adequate for the annihilation of 4T1 cells within a concentration threshold deemed non-toxic in the absence of light. Intriguingly, we discovered that concentrations surpassing 0.6 μg mL^{-1} could elicit a potent cytotoxic effect on 4T1 cells following a mere 5 min of illumination (Fig. 1d), effectively suppressing the viability of half the cell population. Furthermore, the dark toxicity of RDIR780 at equivalent concentrations was discernibly lower than that of DIR780, a phenomenon potentially ascribed to the enhanced biocompatibility endowed by the erythrocyte membrane modification. To graphically juxtapose the dark and phototoxicity profiles of RDIR780, we employed a live/dead cell staining assay to visually appraise the cellular viability under conditions of light exposure *versus* darkness. As depicted in Fig. 1e, red fluorescence, indicative of cellular demise, was scarcely detectable in the non-administered groups, irrespective of light conditions. Conversely, in the groups administered with DIR780 and RDIR780, the non-illuminated group exhibited a broad distribution of green fluorescence with minimal red fluorescence, indicative of commendable dark toxicity. Under illumination, a conspicuous surge in red fluorescence was observed, underscoring the profound cytotoxic impact of post-administration phototherapy on tumor cells.

3.2 PTT-induced immunogenic cell death

Prior studies have elucidated that PTT is capable of triggering ICD in tumor cells, thereby unleashing a cascade of tumor-associated antigens and damage-associated molecular patterns (DAMPs), including calreticulin (CRT), high-mobility group box 1 (HMGB1), and adenosine triphosphate (ATP). The release of these immunomodulatory molecules can expedite the maturation of antigen-presenting cells, such as dendritic cells (DCs), which subsequently present antigens to T lymphocytes, igniting the adaptive immune response. Spurred by these insights, we undertook an assessment of the expression levels of CRT and HMGB1, as well as ATP release in 4T1 cells following PTT induced by DIR780 and RDIR780, employing immunofluorescence and ATP detection assays. Fig. 2a and b reveal that the pronounced green fluorescence encircling the nucleus in the groups treated with DIR780 and RDIR780 in conjunction with laser irradiation is indicative of a significant upregulation of CRT on the surface of 4T1 cells. Additionally, the green fluorescence observed at the nuclear periphery suggests an elevated expression of the HMGB1 protein, particularly when juxtaposed with groups treated with DIR780 and RDIR780 in the absence of laser irradiation. To quantify ATP release, we collected the supernatant from 4T1 cell cultures following a variety of treatment protocols and measured

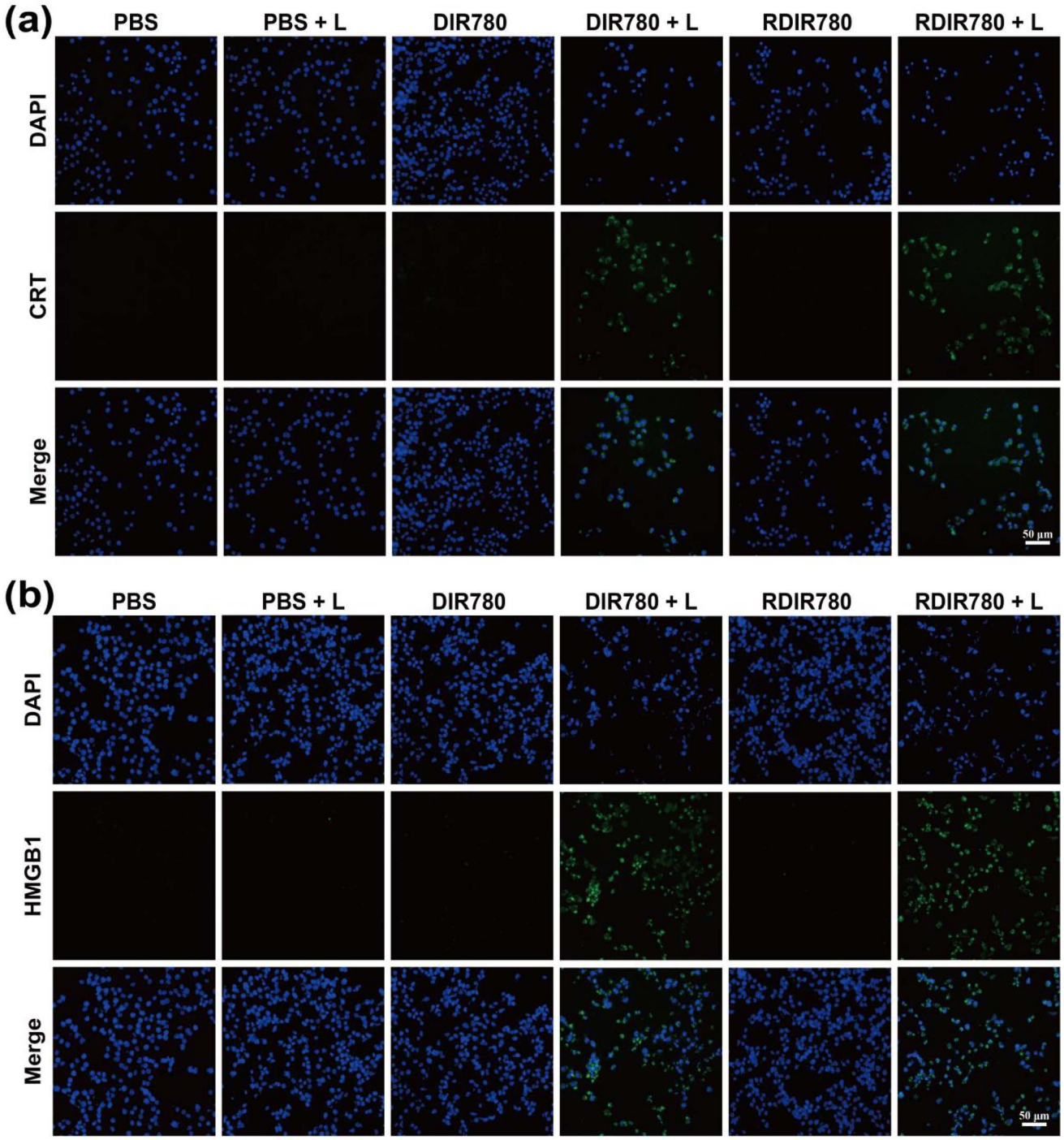

Fig. 2 Immunofluorescence images of (a) CRT and (b) HMGB1 after co-culturing with 4T1 cells and different treatments of DIR780 and RDIR780 (scale: 50 μm).

ATP concentration using an ATP detection kit, as detailed in Fig. S1.† A remarkable increase in ATP content in the 4T1 cell culture medium supernatant was observed subsequent to treatment with DIR780 and RDIR780 accompanied by laser irradiation, markedly divergent from other treatment groups. These compelling findings indicate that PTT mediated by RDIR780 can precipitate ICD in 4T1 cells, thereby underscoring the potential for synergistic immunotherapeutic strategies. This discovery illuminates the capacity of RDIR780 to not only directly assail tumor cells but also to incite the immune system, presenting a convergent approach to cancer treatment that is both targeted and immunologically potent.

3.3 *In vivo* multi-modal imaging

In an endeavor to elucidate the influence of erythrocyte membrane modification on the immune evasion and sustained

circulation of RDIR780 *in vivo*, we utilized fluorescence imaging to track the biodistribution of DIR780 and RDIR780 following tail vein injection in mice. As time progressed post administration, RDIR780 was observed to steadily accumulate at the tumor site, culminating in a peak concentration at the 24 h mark. This critical observation delineates the optimal juncture for laser irradiation therapy, precisely 24 h post injection (Fig. 3a and b). Even at the 96 h interval, RDIR780 continued to exhibit a pronounced fluorescence signal at the tumor site. Comparative analysis with DIR780, as delineated in Fig. S2,† disclosed that RDIR780 manifested a more intense fluorescence at the tumor site, underscoring the erythrocyte membrane's role in curtailing recurrence and extending circulation duration *in vivo*. This enhanced accumulation at the tumor site is instrumental in amplifying the therapeutic impact and potentially reducing the frequency of drug administration.

Capitalizing on the exceptional photothermal efficacy of RDIR780 observed *in vitro*, we advanced our inquiry to evaluate the *in vivo* photothermal conversion efficacy of RDIR780 within tumors. Upon subcutaneous injection at the tumor site of mice bearing 4T1 breast tumors, the animals were subjected to anesthesia, and the tumor region was targeted with laser irradiation, as depicted in Fig. 3c and d. Within the initial minute of laser irradiation, the temperature at the tumor site surged to nearly 50 °C, and further escalated to approximately 60 °C within the subsequent 5 min. Both DIR780 and RDIR780 exhibited remarkable heating capabilities within the murine tumors, thereby highlighting their potential as formidable photothermal agents capable of inducing significant thermal effects at the tumor site. This capability is crucial for the development of effective cancer therapies that can precisely target and eradicate malignant cells.

3.4 *In vivo* anti-tumor performance

In our pursuit to harness the full potential of a synergistic therapeutic approach combining photothermal therapy (PTT) with immunotherapy, we conducted a study using BALB/c mice bearing 4T1 breast tumors. The study was meticulously designed to integrate PTT, directed by RDIR780, with immunotherapy mediated by an anti-PD-L1 antibody. The experimental setup involved seven distinct groups, each receiving

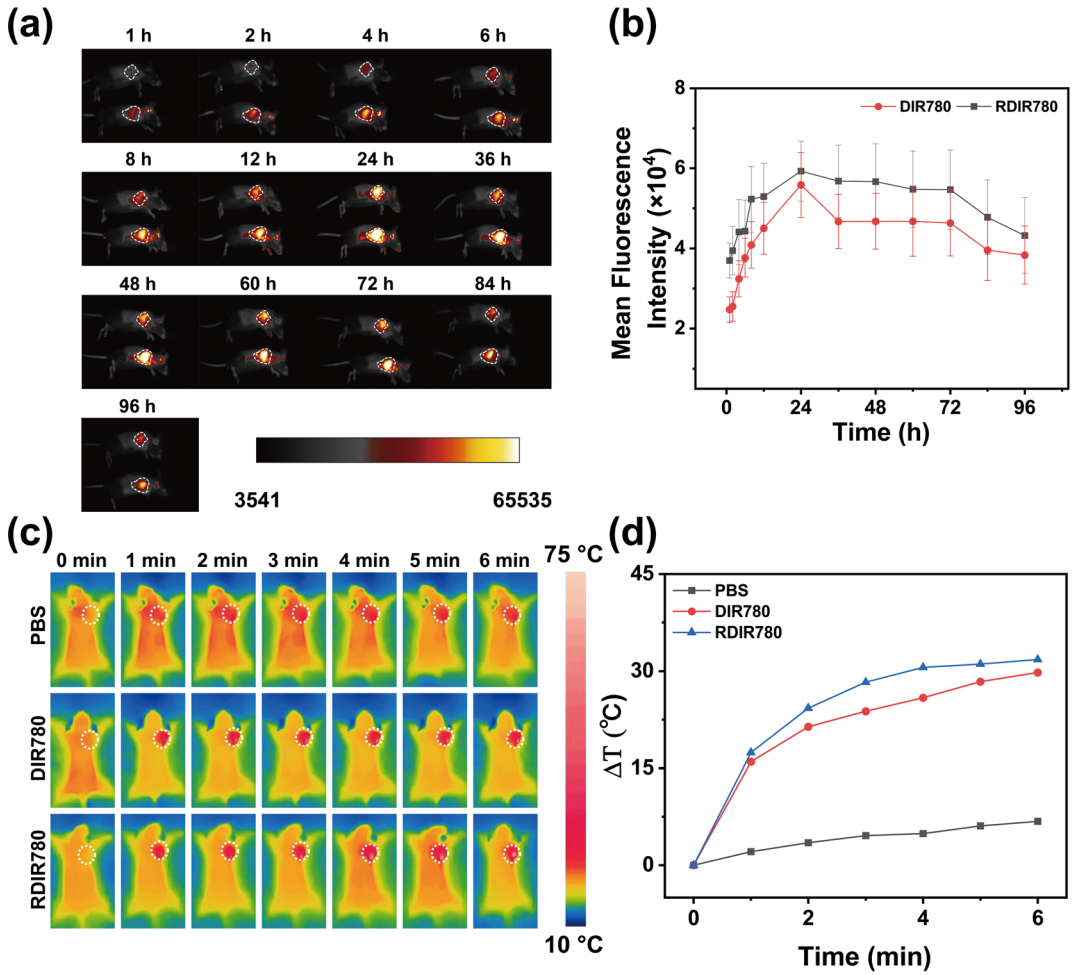

Fig. 3 (a) Changes in fluorescence over time after injection of DIR780 and RDIR780 (200 μL, 60 μg mL^{-1}) into the tail vein of mice. (b) Corresponding average fluorescence intensity change curve for (a). (c) Infrared thermogram of 4T1 tumor bearing mice irradiated with an 808 nm laser (1.0 W cm^{-2}, 6 min) after injection of PBS, DIR780 and RDIR780. (d) Corresponding temperature change curve.

a different treatment regimen: a control group with PBS, anti-PD-L1 antibody alone, DIR780 alone, DIR780 with laser (L) irradiation, RDIR780 alone, RDIR780 with L, and the combination of RDIR780 with anti-PD-L1 antibody and L. The progression of tumor growth was meticulously monitored every two days to assess the effectiveness of each treatment. As depicted in Fig. 4a, groups administered with PBS, anti-PD-L1 antibody, DIR780, and RDIR780 without laser irradiation showed rapid tumor growth, suggesting that these treatments did not effectively inhibit tumor progression. In contrast, groups treated with DIR780 + L and RDIR780 + L exhibited significant suppression of tumor growth, underscoring the substantial inhibitory effects of PTT. Notably, the group treated with RDIR780 + L demonstrated a markedly enhanced antitumor effect compared to the DIR780 + L group. This enhancement is attributed to the immune-evasive properties conferred by the erythrocyte membrane coating, which is hypothesized to prolong the circulation time of RDIR780 *in vivo*, decrease reticuloendothelial system (RES)-mediated clearance, and increase nanoparticle concentration at the tumor sites. Most strikingly, the group treated with the combination of RDIR780 + anti-PD-L1 antibody + L showed an exceptional antitumor response, nearly halting tumor growth entirely. This outcome highlights the significant therapeutic synergy achieved by integrating PTT with immunotherapy, offering a promising strategy for cancer treatment. The synergistic benefits of combining PTT with immunotherapy are manifold: the biomimetic RDIR780 nanoparticles, cloaked in red blood cell membranes, preferentially accumulate at the tumor site due to the EPR effect and active targeting mechanisms, enhancing the effectiveness of PTT. The PTT induced immunogenic cell death (ICD) upregulates the expression of immunostimulatory molecules, facilitating the activation of antigen-presenting cells and T-cell responses. While PTT provides a direct cytotoxic effect on tumor cells, immunotherapy stimulates a systemic immune response, creating a complementary action. This study sets the stage for future investigations into the optimization of such synergistic treatments, offering a promising direction for the development of advanced cancer therapeutics.

Histological analysis of tumor tissues, including hematoxylin and eosin (H&E) staining, TUNEL assay for apoptosis, and Ki67 staining for proliferation (Fig. 4c), revealed that the group treated with the combined therapy exhibited heightened levels of apoptosis and diminished proliferation within the tumor microenvironment, signifying the potent cytotoxic effect against tumor cells and the exceptional antitumor efficacy of the integrated therapeutic approach. Furthermore, as depicted in Fig. 4b and S3,† throughout the 24 day therapeutic journey, the body weight of the mice in all groups experienced only nominal fluctuations, and the routine blood and biochemical indices remained within the normal range. These observations suggest that the treatment did not significantly disrupt the

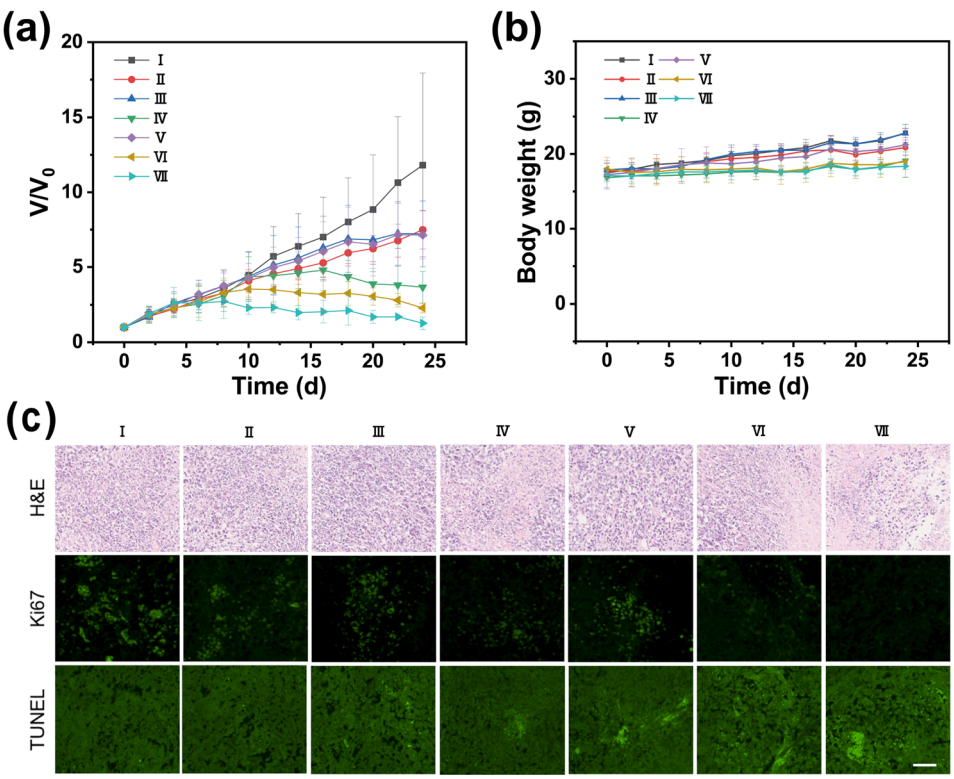

Fig. 4 (a) Ratio of tumor volume to initial volume in 4T1 tumor bearing mice after different treatments. (b) Weight curves of 4T1 tumor bearing mice after different treatments. (c) H&E, Ki67, TUNEL, CRT, and HMGB1 staining of tumor sections obtained from 4T1 tumor-bearing mice. All the scale bars are 100 μm. Group information: (I) PBS, (II) anti-PD-L1 antibody, (III) DIR780, (VI) DIR780 + L (1.0 W cm^{-2}, 6 min), (V) RDIR780, (VI) RDIR780 + L (1.0 W cm^{-2}, 6 min), and (VII) RDIR780 + anti-PD-L1 antibody + L (1.0 W cm^{-2}, 6 min).

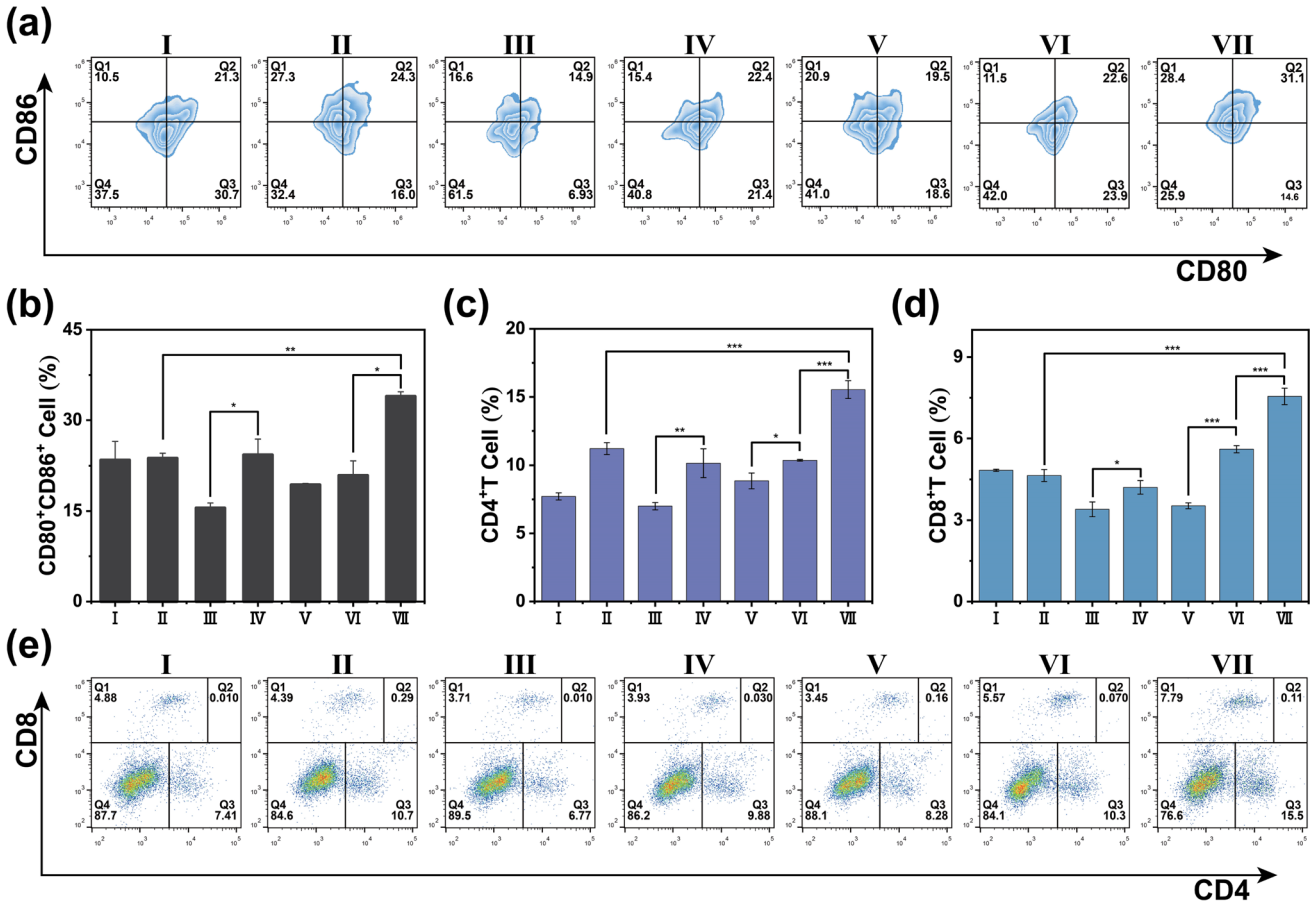

Fig. 5 (a) Maturity status of DCs in different groups of tumor tissues. (b) Statistical chart of $CD80^+CD86^+$T cells. (c) Flow cytometry statistics on the proportion of $CD4^+$T cells in the spleen. (d) Flow cytometry analysis of the proportion of $CD8^+$T cells in the spleen. (e) Flow cytometry analysis of the proportion of $CD4^+/CD8^+$T cells in the spleen. Group information: (I) PBS, (II) anti-PD-L1 antibody, (III) DIR780, (VI) DIR780 + L (1.0 W cm^{-2}, 6 min), (V) RDIR780, (VI) RDIR780 + L (1.0 W cm^{-2}, 6 min), and (VII) RDIR780 + anti-PD-L1 antibody + L (1.0 W cm^{-2}, 6 min).

physiological equilibrium of the mice, thereby confirming the safety and non-toxicity of the administered therapy.

3.5 *In vivo* immune mechanism evaluation

In our pursuit to dissect the intricate immune mechanisms at play when PTT is conjoined with immunotherapy, we conducted a meticulous post-treatment examination of immune parameters in the tumor, spleen, and peripheral blood of representative mice from each experimental group. Dendritic cells (DCs), the quintessential antigen-presenting cells, are central to the orchestration of the immune response, with their functional maturation signaled by the upregulation of $CD80^+$ and $CD86^+$ proteins on their cell surface. Employing flow cytometry, we scrutinized the tumor tissue and discovered a heightened expression of $CD80^+$ and $CD86^+$ in the group subjected to the combined therapy of RDIR780 + anti-PD-L1 antibody + L (Fig. 5a and b). This robust expression is likely a consequence of the formidable photothermal effects induced by RDIR780 + L, which triggers the release of ICD-associated molecular patterns from tumor cells, thus promoting the maturation of DCs. Moreover, the strategic co-administration of the anti-PD-L1 antibody is conjectured to thwart the immune evasion tactics of tumor cells, invigorate the immune system, neutralize the immunogenic substances released by tumor cells, and further catalyze the maturation of DCs. These compelling insights suggest that the fusion of PTT with immunotherapy not only propels the maturation of DCs but also galvanizes the immune system at large. This synergistic activation is pivotal in mounting a comprehensive immune response against the tumor cells, thereby offering a multi-pronged therapeutic strategy to impede cancer progression and amplify treatment efficacy.

The activation of $CD4^+$ and $CD8^+$ T cells is a pivotal hallmark of an invigorated immune response. We meticulously analyzed the T cell populations within the spleen and peripheral blood using flow cytometry. The data presented in Fig. 5c–e, S4 and S5† reveal that the signal intensity for $CD4^+/CD8^+$ T cells in the group subjected to laser irradiation was markedly higher than that in the non-irradiated cohort. More strikingly, the RDIR780 + anti-PD-L1 antibody + L group exhibited an even more pronounced signal for $CD4^+/CD8^+$ T cells, surpassing all other experimental groups, thereby indicating a robust immune system activation. To delve deeper into the systemic immune response, we quantified the serum levels of a spectrum of cytokines through enzyme-

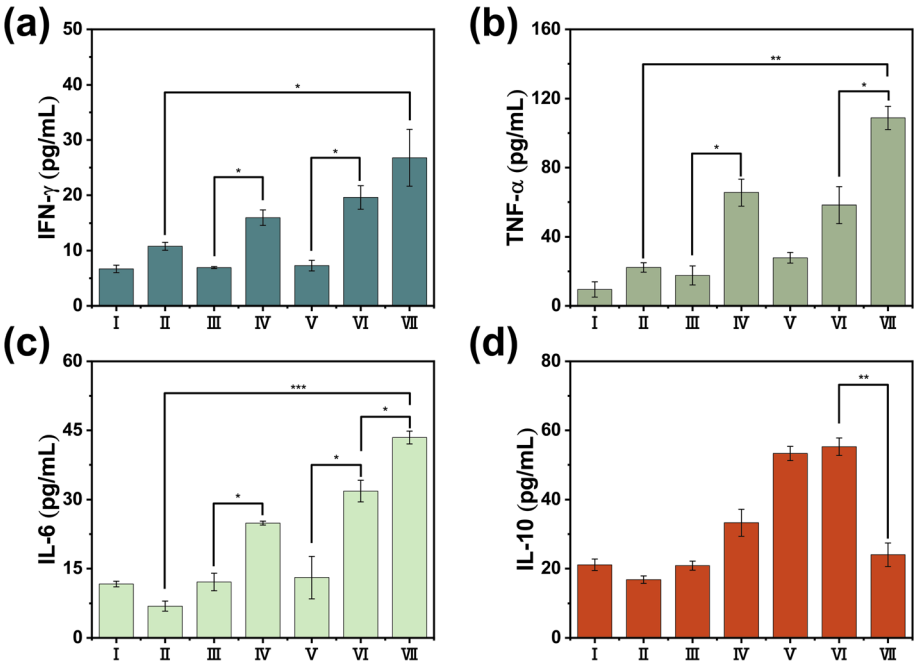

Fig. 6 Secretion levels of (a) IFN-γ, (b) TNF-α, (c) IL-6, and (d) IL-10 in the spleen of 4T1 tumor bearing mice ($n = 3$). Group information: (I) PBS, (II) anti-PD-L1 antibody, (III) DIR780, (VI) DIR780 + L (1.0 W cm^{-2}, 6 min), (V) RDIR780, (VI) RDIR780 + L (1.0 W cm^{-2}, 6 min), and (VII) RDIR780 + anti-PD-L1 antibody + L (1.0 W cm^{-2}, 6 min).

linked immunosorbent assay (ELISA). As illustrated in Fig. 6 and S6,† the concentrations of the pro-inflammatory cytokines TNF-α, IFN-γ, and IL-6 were considerably elevated in the RDIR780 + anti-PD-L1 antibody + L group, while the anti-inflammatory cytokine IL-10 was comparatively diminished. These compelling results suggest that the immunogenic cell death triggered by PTT is instrumental in galvanizing the immune system, and the synergistic application of PTT with immunotherapy elicits a formidable therapeutic impact.

The surface expression of $CD4^+CD25^+$ on T lymphocytes is a signature of regulatory T cells (Treg), which are adept at modulating immune responses. Through flow cytometry, we scrutinized the distribution of $CD4^+CD25^+$ double-positive T lymphocytes among the experimental groups, as shown in Fig. S7 and S8.† The group treated with the anti-PD-L1 antibody displayed a reduced expression level of $CD4^+CD^{25+}$. This finding implies that during the comprehensive activation of the immune system, the tumor's capacity for immune evasion is thwarted, Treg cell differentiation is attenuated, and the dampening effect of Treg cells on the immune response is curtailed. The collective findings underscore that phototherapy, when synergized with the anti-PD-L1 antibody, not only activates the immune system but also effectively precludes the immune evasion of tumor cells. The combination strategy has the potential to reduce the immunosuppressive tumor microenvironment, enhancing the overall efficacy of immunotherapy. This holistic strategy leverages the full spectrum of the immune system's capabilities to confront cancer, presenting a promising horizon for the enhancement of cancer immunotherapeutic strategies.

4. Conclusion

In conclusion, our research has successfully leveraged biomimetic nanoparticles with red blood cell membranes for photothermal synergistic immunotherapy. *In vitro*, RDIR780 nanoparticles have been shown to be efficiently internalized by cells and capable of inducing immunogenic cell death (ICD) in tumor cells under laser irradiation. *In vivo*, these nanoparticles demonstrate prolonged circulation in the bloodstream and effective accumulation at the tumor site, thanks to the red blood cell membrane's immune-evasive properties and the EPR effect. By conjugating RDIR780 with the anti-PD-L1 antibody, we have developed a combined therapy targeting 4T1 breast cancer, integrating PTT with immunotherapy. This strategy not only enhances the therapeutic efficacy but also highlights the potential of erythrocyte membrane-based drug delivery systems in the biomedical field, offering a promising avenue for cancer treatment advancements.

Ethical statement

All animal procedures were performed in accordance with the Guidelines for Care and Use of Laboratory Animals at the Laboratory Animal Center of Hangzhou Normal University and approved by the Animal Ethics Committee of Hangzhou Normal University with a use license number SYXK (Zhejiang) 2020-0026.

Data availability

The data that support the findings of this study are available from the corresponding author upon reasonable request.

Author contributions

Liquan Hong: data curation, methodology, formal analysis. Jingtao Ye: data curation, software, formal analysis. Yang Li: methodology, investigation, funding acquisition, formal analysis, data curation. Shouchun Yin: conceptualization, investigation, writing – review & editing, funding acquisition, project administration.

Conflicts of interest

The authors declare that they have no known competing financial interests or personal relationships that could have appeared to influence the work reported in this paper.

Acknowledgements

This work was supported by the Natural Science Foundation of Zhejiang Province (Grants LZ23B040001, and LY23E030003).

References

1 Y. Li, J. Ye, Y. Li, M. Jiang, T. Shi, H. Qiu and S. Yin, *Polym. Chem.*, 2023, **14**, 3008.
2 M. Jiang, J. Zhang, Y. Li, T. Shi, T. Ma, Y. Sun, H. Qiu, Y. Li and S. Yin, *Mater. Chem. Front.*, 2023, **7**, 3668.
3 H. Zhang, Y. Zhang, Y. Zhang, H. Li, M. Ou, Y. Yu, F. Zhang, H. Yin, Z. Mao and L. Mei, *Nat. Commun.*, 2024, **15**, 6783.
4 M. Ou, C. Lin, Y. Wang, Y. Lu, W. Wang, Z. Li, W. Zeng, X. Zeng, X. Ji and L. Mei, *J. Controlled Release*, 2022, **345**, 755.
5 Y. Zhu, W. R. Archer, K. F. Morales, M. D. Schulz, Y. Wang and J. B. Matson, *Angew. Chem., Int. Ed.*, 2023, **62**, e202302303.
6 C. Lin, C. Huang, Z. Shi, M. Ou, S. Sun, M. Yu, T. Chen, Y. Yi, X. Ji, F. Lv, M. Wu and L. Mei, *Acta Pharm. Sin. B*, 2022, **12**, 4472.
7 O. K. Dagher, R. D. Schwab, S. K. Brookens and A. D. Posey, *Cell*, 2023, **186**, 1814.
8 D. Zhi, T. Yang, J. O'Hagan, S. Zhang and R. F. Donnelly, *J. Controlled Release*, 2020, **325**, 52.
9 Z. Lv, S. He, Y. Wang and X. Zhu, *Adv. Healthcare Mater.*, 2021, **10**, 2001806.
10 J. Zhang, Y. Li, M. Jiang, H. Qiu, Y. Li, M. Gu and S. Yin, *ACS Biomater. Sci. Eng.*, 2023, **9**, 821.
11 H. Li, Y. Li, L. Su, K. Zheng, Y. Zhang, J. Li, F. Lv, M. Huang, T. Chen, H. Zhang, Z. Shi, D. Zhu, X. Dong, W. Zeng and L. Mei, *Adv. Sci.*, 2024, **11**, e2308251.
12 Q. Chen, C. Liu, C. Liu, D. Zhong, S. Hua, J. He, K. Wang and M. Zhou, *Nano Today*, 2021, **41**, 101311.
13 S. A. Rosenberg, J. C. Yang and N. P. Restifo, *Nat. Med.*, 2004, **10**, 909.
14 I. Mellman, G. Coukos and G. Dranoff, Cancer immunotherapy comes of age, *Nature*, 2011, **480**, 480–489.
15 S. Farkona, E. P. Diamandis and I. M. Blasutig, *BMC Med.*, 2016, **14**, 73.
16 H. Wang and D. J. Mooney, *Nat. Mater.*, 2018, **17**, 761.
17 D. Wang, W. Fang, C. Huang, Z. Chen, T. Nie, J. Wang, L. Luo and Z. Xiao, *Smart Mater. Med.*, 2022, **3**, 159.
18 P. Sharma, K. Wagner, J. D. Wolchok and J. P. Allison, *Nat. Rev. Cancer*, 2011, **11**, 805.
19 Y. Yu, Q. Cheng, X. Ji, H. Chen, W. Zeng, X. Zeng, Y. Zhao and L. Mei, *Sci. Adv.*, 2022, **8**, eadd3599.
20 K. Yaddanapudi, R. A. Mitchell and J. W. Eaton, *OncoImmunology*, 2013, **2**, e23403.
21 A. Ribas and J. D. Wolchok, *Science*, 2018, **359**, 1350.
22 D. J. Byun, J. D. Wolchok, L. M. Rosenberg and M. Girotra, *Nat. Rev. Endocrinol.*, 2017, **13**, 195.
23 S. Sheng, X. Yu, G. Xing, L. Jin, Y. Zhang, D. Zhu, X. Dong, L. Mei and F. Lv, *Adv. Funct. Mater.*, 2023, **33**, 2212118.
24 M. H. Pollack, A. Betof, H. Dearden, K. Rapazzo, I. Valentine, A. S. Brohl, K. K. Ancell, G. V. Long, A. M. Menzies, Z. Eroglu, D. B. Johnson and A. N. Shoushtari, *Ann. Oncol.*, 2018, **29**, 250.
25 A. Bhardwaj, J. Kaur, M. Wuest and F. Wuest, *Nat. Commun.*, 2017, **8**, 1.
26 H.-J. Yoon, H.-S. Lee, J.-H. Jung, H. K. Kim and J.-H. Park, *ACS Appl. Mater. Interfaces*, 2018, **10**, 6118.
27 T. Lajunen, L. S. Kontturi, L. Viitala, M. Manna, O. Cramariuc, T. Róg, A. Bunker, T. Laaksonen, T. Viitala, L. Murtomäki and A. Urtti, *Mol. Pharmaceutics*, 2016, **13**, 2095.
28 J. Xiong, M. Wu, J. Chen, Y. Liu, Y. Chen, G. Fan, Y. Liu, J. Cheng, Z. Wang, S. Wang, Y. Liu and W. Zhang, *ACS Nano*, 2021, **15**, 19756.
29 W. Li, T. Ma, T. He, Y. Li and S. Yin, *Chem. Eng. J.*, 2023, **463**, 142495.
30 J. Ye, Y. Yu, Y. Li, B. Yao, M. Gu, Y. Li and S. Yin, *ACS Appl. Mater. Interfaces*, 2024, **16**, 34607.